Supporting Information

Body-centered Cubic Phase in 3-arm Star Mesogens: A Torsional Tapping AFM and GISAXS Study

Christa H. M. Weber,[a] Feng Liu,[b] Xiang-bing Zeng,[b] Goran Ungar,[bc]* Nick Mullin,[a] Jamie K. Hobbs,[a] Michael Jahr,[d] Matthias Lehmann[d]

[a]Department of Physics and Astronomy, University of Sheffield, Hicks Building, Hounsfield Road, Sheffield S3 7RH (UK)

[b]Department of Engineering Materials, University of Sheffield, Mapping Street, Sheffield S1 3JD (UK)

E-mail: g.ungar@sheffield.ac.uk

[c]WCU program of Chemical Convergence for Energy & Environment, School of Chemical and Biological Engineering, Seoul National University, Seoul (Korea)

[d]Institute of Chemistry, Chemnitz University of Technology, Straße der Nationen 62, 09111 Chemnitz (Germany)

1. DSC

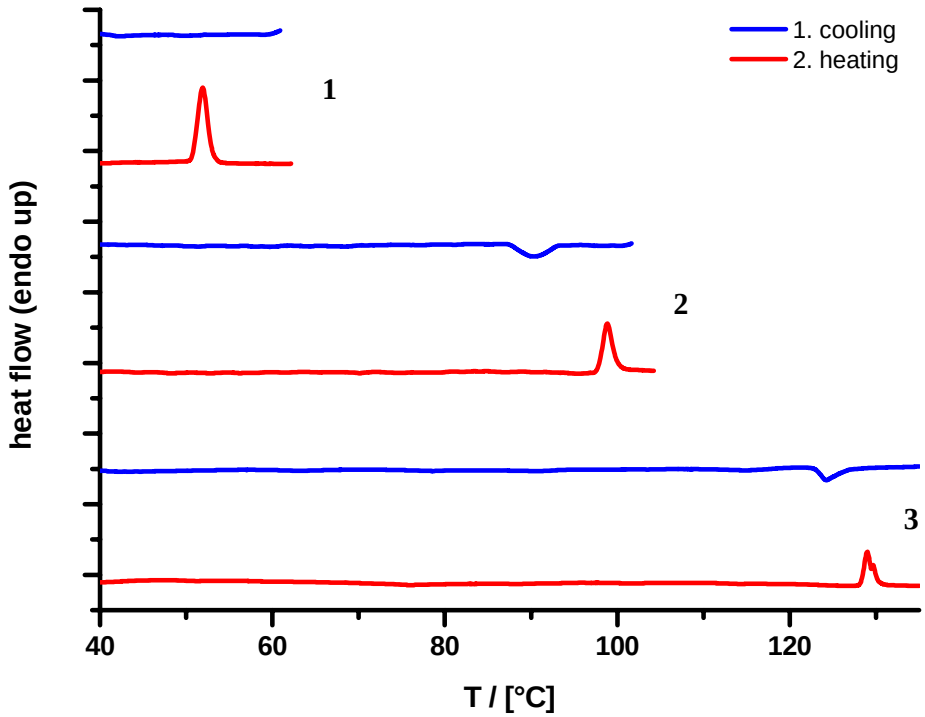

Figure S1. DSC traces of compounds **1, 2** and **3** recorded on heating and cooling.

2. X-ray Diffraction

2.1. Small-angle powder diffraction
High-resolution small- to intermediate angle powder diffraction patterns, simultaneously with wide-angle diffractograms, were recorded at Station I22 of Diamond Light Source, UK. Samples were held in evacuated 1 mm capillaries which were held in a modified Linkam hot stage, which had a hole drilled through the silver heating block and mica windows attached to the block on each side. A RAPID2 area detector was used for small to intermediate angles, and wide-angle diffractograms were recorded using the HotWAXS curved position-sensitive detector developed by the Daresbury Detector Group. Azimuthal integration was performed using FibreFix, part of the CCP13 suite. *q* calibration and linearization were verified using several orders of layer reflections from a series of crystalline orthorhombic *n*-alkanes. Diffraction intensities were Lorentz and multiplicity corrected.

22. Grazing incidence small angle scattering (GISAXS)
GISAXS experiments were performed on the XMaS beamline (BM28) at the ESRF in Grenoble. A purpose-built temperature-controlled sample stage, a He-flushed sample chamber, and a MarCCD detector were used, as described in ref. **Error! Bookmark not defined.**4. GISAXS was recorded both below and above the critical angle to distinguish any possible differences between the surface and the bulk of the film.

2.3. Electron density reconstruction

The electron density of a liquid crystal in the unit cell $\rho(x,y,z)$ is related to the structure factor $F(hkl)$ by Fourier transformation:

$$\rho(x,y,z) = \frac{1}{V}\sum_{hkl} F(hkl)\exp[-2\pi i(hx+ky+lz)]$$

$F(hkl)$ is in turn related to the intensity of the (hkl) reflection $I(hkl)$ as
$I(hkl) = \text{const.} \times |F(hkl)|^2$
Thus the electron density $\rho(x,y,z)$ can be reconstructed from the intensities of x-ray reflections $I(hkl)$ using the general formula:

$$\rho(x,y,z) = \frac{1}{const.}\sum_{hkl}\sqrt{I(hkl)}\exp[-2\pi i(hx+ky+lz)+i\phi_{hkl}]$$

Here ϕ_{hkl} is the phase angle of the structure factor $F(hkl)$.

The diffraction intensities of the cubic phase, measured from the powder diffraction data of compound **1** are provided in Table S1.

Table S1. Indices, experimental and calculated *d*-spacings, and intensities of x-ray diffraction peaks observed for compound **1** at 20 ºC. The phases used for electron density map reconstruction are also listed.

Indices	*d*-spacings (nm)		Intensities	Phases
	Experimental	calculated a = 4.94 nm		
(110)	3.49	3.49	100	0
(200)	2.47	2.47	0.49	π
(211)	2.02	2.02	4.82	π
(220)	1.75	1.75	1.68	π

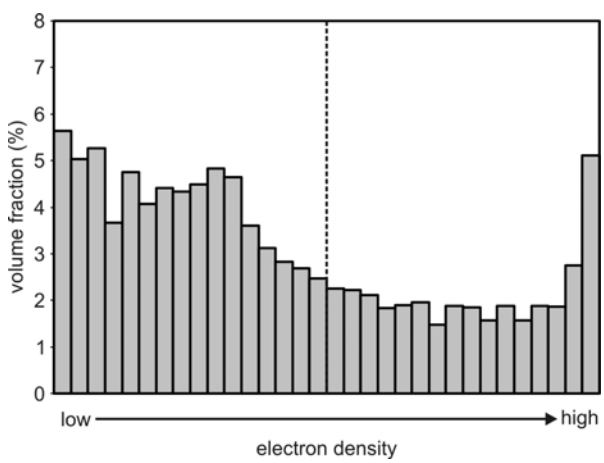

Figure S2. Histogram of the reconstructed electron density map. The level of the isoelectron surface used in Figure 5 is indicated by the dashed vertical line, which corresponds to the boundary between the low electron density aliphatic regions (70% of total volume) and the high density aromatic regions (30% of total volume).

3. Molecular Simulation

Annealing dynamics runs were carried out using the Forcite + module and the Universal Force Field (Material Studio, Accelrys). The structures in Figure 6 was obtained with 13 molecules, as shown in Table 3 of ref. 18, in a cubic box with the length determined by experiment, with 3-d periodic boundary conditions. 400 temperature cycles of NVT dynamics were run between 300 and 700 K, with a total annealing time of 0.4 ns. Additionally, attempts were made to run annealing dynamics on a unit cell containing two clusters centered at (0, 0, 0) and (½, ½, ½), equivalent to a BCC structure. However, the simulation was too slow to be practical.

4. Optical Microscopy

The samples were prepared on glass slides and observed under an Olympus BX51 optical microscope using the interference contrast mode. A Linkam heating cell was used to cool the sample very slowly (0.01 ºC/min) from the isotropic state in order to form the faceted droplets. Images were captured using a CoolSNAP digital camera (Roper Scientific), which is linked to a desktop PC and controlled by the Image-Pro Plus software (Media Cybernetics).